J Biol Inorg Chem (2001) 6: 763–769
DOI 10.1007/s007750100252

ORIGINAL ARTICLE

Boris Bleijlevens · Bart W. Faber · Simon P.J. Albracht

# The [NiFe] hydrogenase from *Allochromatium vinosum* studied in EPR-detectable states: H/D exchange experiments that yield new information about the structure of the active site

Received: 6 February 2001 / Accepted: 8 April 2001 / Published online: 14 June 2001


**Abstract** In this study we report on thus-far unobserved proton hyperfine couplings in the well-known EPR signals of [NiFe] hydrogenases. The preparation of the enzyme in several highly homogeneous states allowed us to carefully re-examine the $Ni_u$*, $Ni_r$*, $Ni_a$-C* and $Ni_a$-L* EPR signals which are present in most [NiFe] hydrogenases. At high resolution (modulation amplitude 0.57 G), clear indications for hyperfine interactions were observed in the $g_z$ line of the $Ni_r$* EPR signal. The hyperfine pattern became more pronounced in $^2H_2O$. Simulations of the spectra suggested the interaction of the Ni-based unpaired electron with two equivalent, non-exchangeable protons ($A_{1,2} = 13.2$ MHz) and one exchangeable proton ($A_3 = 6.6$ MHz) in the $Ni_r$* state. Interaction with an exchangeable proton could not be observed in the $Ni_u$* EPR signal. The identity of the three protons is discussed and correlated to available ENDOR data. It is concluded that the NiFe centre in the $Ni_r$* state contains a hydroxide ligand bound to the nickel, which is pointing towards the gas channel rather than to iron.

**Keywords** [NiFe] hydrogenase · EPR spectroscopy · Redox states · Active site · Hydrogen/deuterium exchange

## Introduction

[NiFe] hydrogenases catalyse the reversible oxidation of molecular hydrogen into two protons and two electrons. Presently, the crystal structures of five [NiFe] hydrogenases have been determined. The active site consists of two metal ions, one Ni and one Fe, bound to the protein via four cysteine thiols [1]. The valence state of the Ni ion usually shuttles between II and III. The Fe remains in a low-spin Fe(II) state [2, 3] and binds three unusual ligands, two cyanides and one carbon monoxide [4, 5, 6]. Exchange experiments showed that the splitting of dihydrogen is heterolytic [7]. The proton that is the result of this splitting is transferred via a proton channel to the outside of the molecule. The hydride produced is oxidized and the electrons are transferred via one or more Fe-S clusters to an electron-acceptor site.

Most [NiFe] hydrogenases are reversibly inactivated by oxygen. This enables aerobic purification of these enzymes. The inactivated enzyme can be reactivated by a process that has become known as ''reductive activation''. This is normally carried out by incubation under a hydrogen gas atmosphere. For *Allochromatium vinosum* [NiFe] hydrogenase, this procedure consists of a 30 min incubation under 100% $H_2$ at 50 °C. Studies on the properties of [NiFe] hydrogenases have revealed that they can exist in a number of states, distinguishable by EPR and FTIR spectroscopy (for an overview see [8]).

EPR studies on the enzymes from *Desulfovibrio gigas* and *A. vinosum* showed that there are two EPR-detectable, inactive, oxidized states. The first state, with $g_{xyz} = 2.31, 2.24, 2.01$, represents an unready form of the enzyme as it takes at least 1 h at room temperature to show activity with hydrogen. This state is termed $Ni_u$* (u for ''unready''; * for an $S = 1/2$ system) or Ni-A. The second state, with $g_{xyz} = 2.33, 2.16, 2.01$, is termed $Ni_r$* (r for ''ready'') or Ni-B as it readily activates with hydrogen [9]. The EPR-detectable, reduced form of the enzyme was termed $Ni_a$-C* ($g_{xyz} = 2.21, 2.15, 2.01$; a for ''active''). This state is light sensitive at cryogenic temperatures and is then converted to the $Ni_a$-L* state with $g_{xyz} = 2.28, 2.11, 2.045$ [10].

Re-oxidation of the active enzyme with $^{17}O_2$ showed that in both the $Ni_r$* as well as the $Ni_u$* states an oxygen species is close to the unpaired electron on nickel since the $I = 5/2$ nucleus of $^{17}O$ caused line broadening of both EPR signals [11]. In the crystal structure of as-isolated,

B. Bleijlevens · B.W. Faber · S.P.J. Albracht (✉)
Swammerdam Institute for Life Sciences, Biochemistry,
University of Amsterdam, Plantage Muidergracht 12,
1018 TV Amsterdam, The Netherlands
E-mail: a311siem@chem.uva.nl
Tel.: +31-20-5255130
Fax: +31-20-5255124

oxidized *D. gigas* hydrogenase a patch of electron density, observed between the nickel and the iron, was attributed to a bridging oxygen species [4]. The crystal structure of reduced, active [NiFeSe] hydrogenase from *Desulfomicrobium baculatum* did not show this electron density [12]. The oxidized *D. gigas* hydrogenase used to obtain crystals was a mixture of several forms of the enzyme [1]. EPR analysis of the crystals showed that 50% of the Ni sites were EPR silent. From the remaining half, 85% was in the $Ni_u$* and 15% was in the $Ni_r$* state. The EPR-silent enzyme molecules were not in an active or ready form since development of full hydrogenase uptake activity required hours of incubation under 100% $H_2$. Up till now, it has not been possible to obtain the *D. gigas* enzyme solely in the $Ni_u$* or $Ni_r$* state. *A. vinosum* hydrogenase is spectroscopically very similar to the *D. gigas* enzyme, but it can be manipulated into either the $Ni_r$* or the $Ni_u$* state for more than 95% of the sites.

Electron-nuclear double resonance (ENDOR) measurements on *A. vinosum* hydrogenase in the $Ni_r$* state revealed the interaction of four protons with the Ni-based unpaired electron [13]. Two protons with a mainly isotropic coupling of 12.6 and 12.5 MHz were assigned to belong to the $\beta$-$CH_2$ group of a bridging cysteine residue (equivalent to Cys533 in the *D. gigas* structure). A third proton (coupling mainly anisotropic, 3.5 MHz) was considered to be the closest proton of the $\beta$-$CH_2$ of the second bridging cysteine residue (Cys68) or a thiol proton on one of the terminal cysteine residues (Cys65 or Cys530). Interaction with a fourth nucleus was observed only in the high-field region of the spectrum, near $g = 2.01$. This coupling was obscured by the strong absorption of the $[3Fe\text{-}4S]^+$ cluster in this region at 10 K. A coupling constant of $\sim$6 MHz was estimated and tentatively assigned to be caused by the methyl group of Val67.

In this paper we studied the effect of exchangeable protons on the EPR signals of the Ni site in the inactive oxidized $Ni_r$* and $Ni_u$* states. We found that the 6 MHz coupling is from an exchangeable proton; the coupling is anisotropic and only observed in the $Ni_r$* state.

## Materials and methods

### Purification

*A. vinosum* DSM 185 was grown in a 700 L batch culture [14] in a medium essentially as described previously [15, 16]. The membrane-bound [NiFe] hydrogenase was isolated and purified as described [17]. The $F_{420}$-nonreducing hydrogenase from *Methanothermobacter marburgensis* (formerly *Methanobacterium thermoautotrophicum* strain Marburg) was a gift from Dr. R. Hedderich (Marburg, Germany).

### EPR spectroscopy

X-band EPR spectra were recorded on a Bruker ECS 106 spectrometer. The modulation frequency was 100 kHz. Cooling of the sample was performed using an Oxford Instruments ESR 900 cryostat with an ITC4 temperature controller. The magnetic field was calibrated with an AEG magnetic field meter. The microwave frequency was measured with an HP 5244A frequency converter. The modulation amplitude was 0.57 G.

### Simulations of EPR spectra

Spectra were simulated using home-made programs based on formulas published by Beinert and Albracht [18]. For the simulation of a separate $g_z$ line of a rhombic spectrum, this line was treated as an inverse, absolute, isotropic signal with hyperfine interaction with two or three $I = 1/2$ nuclei. The resultant line shape was compared with the experimental $g_z$ lines. This method enabled rather accurate values for coupling constants ($A$) and line widths ($W$).

### Preparation of the redox states

The two oxidized, inactive states, the $Ni_u$* (Ni-A) and the $Ni_r$* (Ni-B) states, were produced at high homogeneity in buffers prepared with either $H_2O$ or $D_2O$. In $D_2O$, pD values were pH + 0.41. For the $Ni_u$* state, the enzyme in a 10 mM MES/CAPSO buffer (pH 6.0) (MES = 2-morpholinoethanesulfonic acid; CAPSO = 3-cyclohexylamino-2-hydroxy-1-propanesulfonic acid) was incubated under 100% $H_2$ at 50 °C for 30 min in a septum-capped bottle. The reduced, activated enzyme was incubated under 100% carbon monoxide (10 min at room temperature) and subsequently oxidized at 50 °C by slowly allowing air into the bottle via a thin needle. The $Ni_r$* state was prepared in 10 mM MES/CAPSO buffer (pH 9.0). The enzyme was activated as described above, but then it was re-oxidized quickly by a 10-fold dilution in an ice-cold, oxygen-saturated buffer. The $Ni_a$-C* state was prepared in 50 mM MES buffer (pH 6.5) by activation (as described above) and subsequent incubation under a mixture of 1% $H_2$ and 99% He for 15 min at room temperature. The $Ni_a$-C* state was converted to the $Ni_a$-L* state by illumination of the samples at 30 K [10]. During incubations the samples were stirred to optimize gas exchange. After oxidation, 20% glycerol was added to the $Ni_u$* and $Ni_r$* samples to minimize freezing artefacts.

## Results

The *A. vinosum* [NiFe] hydrogenase was prepared in four EPR-detectable states ($Ni_u$*, $Ni_r$*, $Ni_a$-C* and $Ni_a$-L* [8]). The effect of exchangeable protons on EPR spectra recorded with modulation amplitudes of 0.57 G was studied.

The $Ni_u$* state in $H_2O$ showed a rhombic spectrum. The $g$ values were 2.312, 2.237 and 2.013 ($g_{xyz}$) with apparent line widths of 15.6, 10.9 and 4.8 G ($W_{xyz}$) at a modulation amplitude of 0.57 G (Fig. 1A). Close inspection of the separate $g$ values showed a faintly resolved hyperfine splitting in the $g_z$ line only (Fig. 2D). A similar, better resolved, splitting was observed in the $g_z$ line of the EPR spectrum of the $F_{420}$ nonreducing hydrogenase from *M. marburgensis* in the $Ni_u$* state (Fig. 2D). In neither of the two enzymes did the $g_x$ or the $g_y$ line show similar resolved couplings. The spectrum of the $Ni_u$* state of *A. vinosum* hydrogenase prepared in $D_2O$ was, apart from a small increase in the width of the $g_y$ line, the same as in $H_2O$ (Table 1). The faint shoulders in the $g_z$ line were unaltered, showing that they are not due to exchangeable protons (Fig. 2D).

The enzyme in the $Ni_r$* state prepared in $H_2O$ showed an EPR signal with $g$ values at 2.330, 2.160 and 2.008

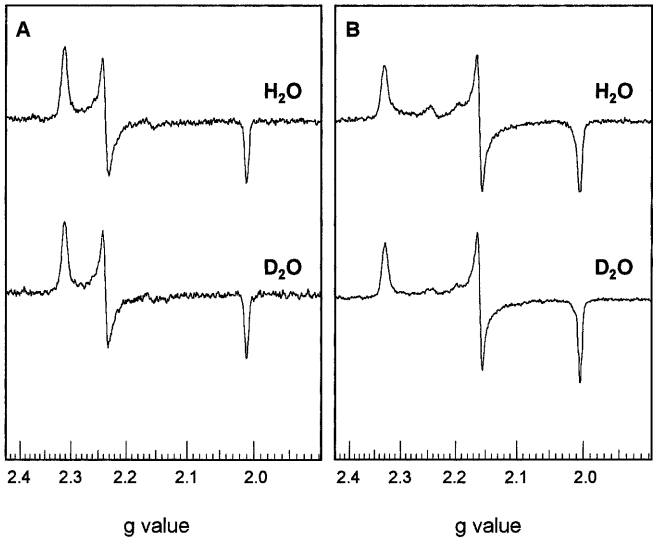


**Fig. 1A, B** EPR spectra of *A. vinosum* [NiFe] hydrogenase in the oxidized states in $H_2O$ and $D_2O$. **A** Enzyme in the $Ni_u$* state. **B** Enzyme in the $Ni_r$* state. EPR conditions: microwave frequency, 9424 MHz (**A**), 9423 MHz (**B**); temperature, 70 K; power, 2 mW; modulation amplitude, 0.57 G

($g_{xyz}$) with line widths of 16.5, 10.9 and 3.1 G (Fig. 1B). A faintly resolved splitting in the $g_z$ line was observed. In $D_2O$ this splitting was much better resolved (Fig. 2C), indicating the removal of the contribution of one or more exchangeable protons. The other two lines ($g_x$ and $g_y$) did not show any signs of coupling to exchangeable protons. When in the $Ni_r$* state in $D_2O$ the buffer was exchanged for $H_2O$, the EPR spectrum remained

**Fig. 2A–D** Detailed view of the EPR spectra of *A. vinosum* [NiFe] hydrogenase in $H_2O$ (*top*) and in $D_2O$ (*middle*). Subtractions of these spectra are shown at the *bottom*. **A**, **B** and **C**: $g_x$, $g_y$ and $g_z$ regions of the $Ni_r$* state. **D**: $g_z$ region of the $Ni_u$* state of *A. vinosum* in $H_2O$ (*top*) and $D_2O$ (*middle*) and the $g_z$ region of the $F_{420}$ nonreducing [NiFe] hydrogenase from *M. marburgensis* in $H_2O$ (*bottom*). All three spectra in **D** are averages of six measurements. EPR conditions for all traces: microwave frequency, 9425 MHz; temperature, 70 K; power, 2 mW; modulation amplitude, 0.57 G

**Table 1** $g$ values and apparent line widths (in G) for EPR signals of the $Ni_u$* and $Ni_r$* states prepared in either $H_2O$ or $D_2O$[a]

| | $g_x$ | $W_x$ | $g_y$ | $W_y$ | $g_z$ | $W_z$ |
|---|---|---|---|---|---|---|
| $Ni_u$* ($H_2O$) | 2.312 | 15.6 | 2.237 | 10.9 | 2.013 | 4.8 |
| $Ni_u$* ($D_2O$) | 2.312 | 15.6 | 2.237 | 12.2 | 2.013 | 4.8 |
| $Ni_r$* ($H_2O$) | 2.330 | 16.5 | 2.160 | 10.9 | 2.008 | 3.1 |
| $Ni_r$* ($D_2O$) | 2.330 | 15.5 | 2.160 | 9.8 | 2.008 | 3.1 |

[a]Spectra were recorded under non-saturating conditions (temperature, 70 K; microwave power, 2 mW; modulation amplitude, 0.57 G). Data based on simulations of whole spectra except for $W_z$, which is based on simulations of the $g_z$ region only and accounting for magnetic interaction with proton nuclei (for details see Fig. 3)

unchanged (results not shown). This showed that it was not possible to exchange incorporated deuteron(s) with bulk proton(s) once the enzyme was in the oxidized state.

In order to better understand the nature of the detectable couplings in the $g_z$ region, the signals were simulated. The $g_z$ line of the EPR spectrum of $Ni_r$* in $D_2O$ could be simulated with a width ($W_z$) of 3.1 G plus a splitting by two equivalent nuclei ($I=1/2$) with a coupling constant ($A_{1,2}$) of 4.7 G (Fig. 3B). In order to simulate the $g_z$ region of $Ni_r$* in $H_2O$, an additional coupling ($I=1/2$) with $A_3=2.35$ G was required to optimally fit the shape of this $g_z$ line (Fig. 3A). Comparison of the spectra of $Ni_r$* in $H_2O$ and in $D_2O$ showed that the hyperfine coupling from the exchangeable proton is mainly anisotropic since it was observed only in the $z$ direction (Fig. 2). The line widths in the $x$ and $y$ directions did not change upon H/D exchange and so no isotropic hyperfine interaction could be detected for this proton.

The distance ($r$) between an unpaired electron and a satellite nucleus can be estimated from their dipolar (anisotropic) interaction according to:

$$A_{\mathrm{dip}} = (\beta_e g_e \beta_N g_N / h)(\rho / r^3) \quad (1)$$

In this formula, $A_{\mathrm{dip}}$ is the dipolar part of the coupling, $\beta_e$ is the Bohr magneton, $g_e$ is the electron $g$ factor, $\beta_N$ is the nuclear magneton, $g_N$ is the $g$ factor of the nucleus

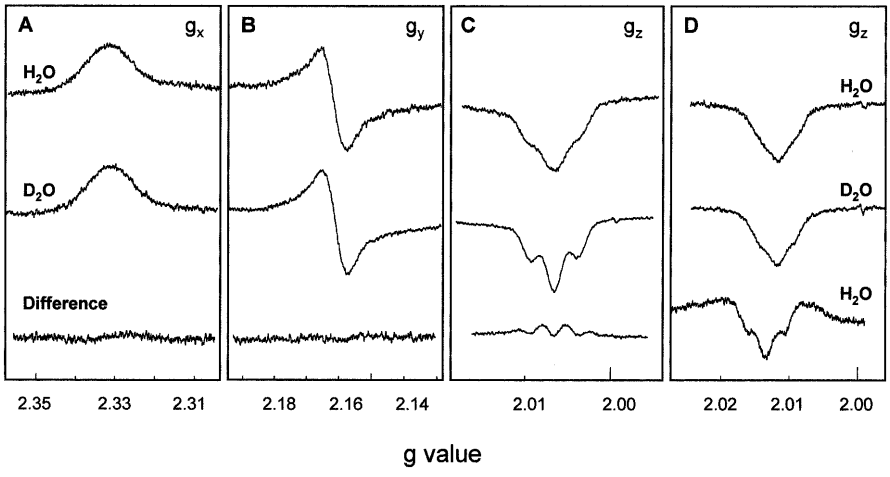

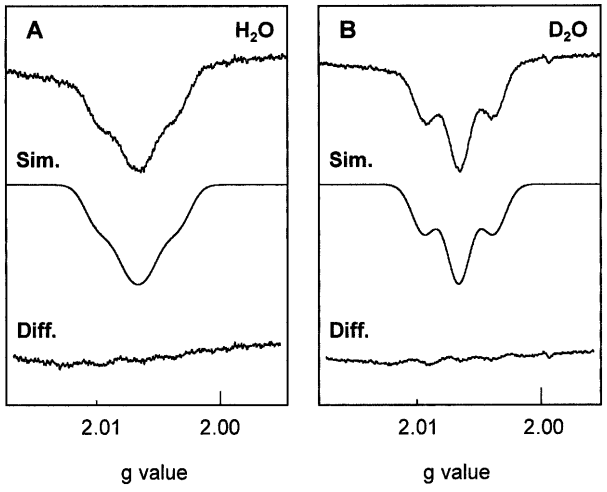


**Fig. 3** Simulations of the $g_z$ region of the EPR spectrum of the $Ni_r$* state from *A. vinosum* hydrogenase prepared in $H_2O$ (**A**) and in $D_2O$ (**B**). *Top*: experimental spectra at 0.57 G modulation amplitude. *Middle*: simulations. Parameters for the enzyme in $H_2O$: $W_z = 3.1$ G with three $I = 1/2$ nuclei ($A_{1,2} = 4.7$ G, $A_3 = 2.35$ G). Parameters for the enzyme in $D_2O$: $W_z = 3.1$ G with two nuclei $I = 1/2$ ($A_{1,2} = 4.7$ G). The expected hyperfine contribution (about 0.4 G) of a $^2H$ nucleus, replacing the $^1H$ nucleus, was neglected. *Bottom*: difference of the experimental minus the simulated spectra

and $h$ is Planck's constant. Assuming an unpaired spin density on the Ni nucleus ($\rho$) of 1, a dipolar coupling of 2.35 G can be caused by a proton at a distance of 2.3 Å. The results of theoretical studies predict variable spin densities on nickel: one study locates almost all of the unpaired spin density at the Ni ion in the $Ni_r$* state [19], while another study shows that in this state only about half of the unpaired spin density is located on the Ni ion [20]. In this latter case the estimated distance would be smaller (1.7 Å).

Apart from the oxidized states, also the two EPR-detectable reduced states ($Ni_a$-C* and $Ni_a$-L*) were subjected to the same analysis. Similar experiments have already been published [11] but in these studies a modulation amplitude of 6 G was used. Therefore, we decided to repeat these experiments using a significantly smaller modulation amplitude (2.26 G). This did not reveal any previously unobserved couplings and, as reported before, the line narrowing, especially in the $Ni_a$-C* state, was considerable upon H/D exchange (results not shown). In previous ENDOR studies, weak proton hyperfine couplings were observed [21, 22], but owing to the broadness of the EPR lines these couplings remained unresolved in our spectra also at higher resolutions.

## Discussion

### Magnetic properties

The EPR signals for the oxidized and the reduced states of [NiFe] hydrogenases are long known and well studied. Careful analysis, however, showed a previously unobserved, small coupling by two nuclei in the $g_z$ line of the $Ni_u$* EPR signal. In the *A. vinosum* enzyme this coupling is hard to detect as the $g_z$ is intrinsically too broad ($W_z = 4.8$ G). In the *M. marburgensis* hydrogenase however, the $g_z$ line is more narrow, making the coupling more pronounced (Fig. 2D). The experiments show that this coupling is not caused by exchangeable protons, since the spectrum of the $Ni_u$* state of *A. vinosum* enzyme prepared in $D_2O$ did not change (Fig. 2D).

The enzyme in the $Ni_r$* state prepared in $D_2O$ showed a clear splitting at the $g_z$ line from two equivalent $I = 1/2$ nuclei (Fig. 2C). In $H_2O$ this coupling was obscured by an extra hyperfine splitting of an exchangeable proton, making the difference spectrum non-zero (Fig. 2C). It was not possible to exchange the incorporated deuteron for a proton when the enzyme was in the oxidized state.

The results of the simulations of the $g_z$ line (Fig. 3) are in good agreement with a recent ENDOR study on the [NiFe] hydrogenase of *A. vinosum* in the $Ni_r$* state [13]. In this study, two large, predominantly isotropic, couplings (12.5 and 12.6 MHz) were attributed to the $\beta$-$CH_2$ protons (H1 and H2) of a bridging Cys residue (Cys533 in the *D. gigas* enzyme). These values correspond well to the observed splittings of $g_z$ of the $Ni_r$* spectrum by H1 and H2 in our study (4.7 G equals a coupling constant of 13.2 MHz at $g = 2.008$). It has been shown by single-crystal EPR on *D. vulgaris* Miyazaki F hydrogenase that the $z$-axis of the $g$ tensor is oriented towards this bridging Cys residue [23]. Since the $g_z$ line of the EPR spectrum of $Ni_r$* is intrinsically narrow, it is possible to detect the coupling in this direction.

Geßner and co-workers for the first time identified a proton (labelled M in [13] and H4 here) interacting with the unpaired electron on nickel in the $Ni_r$* state with an estimated coupling constant of ~6 MHz. The ENDOR signals observed at 10 K were located only near the $g_z$ line where the signal of the $[3Fe\text{-}4S]^+$ cluster absorbs very strongly; hence no proper assignment could be made. Our results, obtained at 70 K, at which temperature the $[3Fe\text{-}4S]^+$ cluster does not interfere, suggest that this coupling must be due to an exchangeable proton. Simulation of the $g_z$ line of the $Ni_r$*($H_2O$) spectrum required a third proton, coupling with a magnitude of 2.35 G (6.6 MHz at $g = 2.008$), in order to properly mimic the experimental spectrum. The magnitude of this coupling and its anisotropy indicate that the exchangeable proton observed in our experiment is the same one as detected by ENDOR spectroscopy.

ENDOR studies also identified a much smaller coupling to the Ni-based unpaired electron in the enzyme in the oxidized ready state. This proton (H3), with a coupling constant of 3.5 MHz (approximately 3 MHz anisotropic), could not unequivocally be assigned. The maximum coupling appears near $g_x = 2.33$, which makes an orientation of the dipolar axis close to the $x$-axis probable [13]. Fan and co-workers [21] showed that this proton was exchangeable and suggested it to be near to the Ni ion as a bound water molecule or a hydroxide. Geßner and co-workers [23] could not reject this inter-

pretation but favoured the closest of the $\beta$-$CH_2$ protons of the second bridging cysteine residue (Cys68), which is positioned in the direction of the *x*-axis. This proton fitted a minimal distance of 3 Å to the Ni site. We do not think, however, that this proton would be exchangeable. Alternatively, they considered a proton bound to one of the terminal cysteine residues (Cys530 or Cys65) to couple to the $S = 1/2$ Ni site at this frequency. Based on arguments discussed in the following section, we prefer H3 to be a proton on the sulfur of Cys530, which is also directed along the *x*-axis.

## Structural implications

The coupling of an exchangeable proton (H4) in the $Ni_r$* state, and the anisotropy thereof, obviously has implications for the active site structures in the oxidized states. In the crystal structure of *D. gigas* hydrogenase, a patch of electron density bridging the Ni and the Fe atom was assigned to an oxygen species. It should be mentioned that the crystal structure was obtained from a mixture of different enzyme redox states (50% EPR silent, 42.5% $Ni_u$* and 7.5% $Ni_r$* [1]). This limits a proper assignment of the bridging oxygen to a certain state. EPR studies of *A. vinosum* enzyme oxidized with $O_2$ enriched in $^{17}O$ ($I = 5/2$) had already shown that an oxygen species must be present close to nickel in both the $Ni_u$* and the $Ni_r$* states, since considerable line broadening was observed for both [11]. However, the exact identity of the oxygen species remained unclear. Possible candidates include $O^{2-}$, $OH^-$ and $H_2O$. For the $Ni_r$* state a hydroxide ligand ($OH^-$) would explain both the $^{17}O$ coupling [11] and the coupling of the exchangeable proton found in this study. The anisotropy of the proton coupling suggests that it is positioned in the direction of the *z*-axis (Fig. 4A). In the crystal structure this axis runs from the bridging Cys533 to the empty ligand site facing the gas channel [23, 24]. A crystallographic study on the *D. vulgaris* Miyazaki F enzyme showed that this is also the binding place for exogenous CO [25].

An EPR analysis of model compounds [26] supports the theory that the unpaired electron, in a low-spin $3d^7$ system with $g_z \approx 2$, is occupying the $d_{z2}$ orbital [27]. In this study a series of Ni(III) complexes of the general formula $Ni[C_6H_3(CH_2NMe_2)_2\text{-}o,o]X_2$, with X = Cl, Br or I, was analysed. The crystal structure of the iodide complex was determined and showed a distorted, square-pyramidal coordination with a halide in an apical position and two nitrogens, one carbon and one halide in the equatorial plane. The 9 GHz EPR spectrum of the chloro compound ($g_{xyz} = 2.366$, 2.190, 2.020) showed a four-fold splitting in the $g_z$ line due to coupling to the apical chloride ($I = 3/2$). EPR spectra of the bromo and the iodo compounds at 35 GHz also showed a four-fold splitting restricted to the $g_z$ direction (S.P.J. Albracht, D.M. Grove and G. van Koten, unpublished results). The equatorial halide and nitrogens did not show resolved hyperfine interactions with the unpaired electron

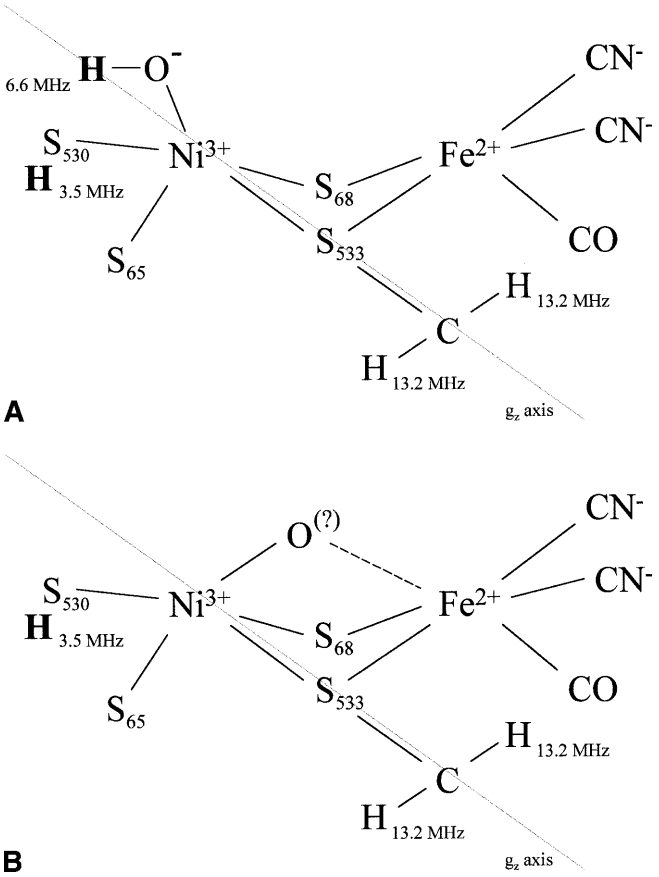


**Fig. 4A, B** Proposed active site structures for *A. vinosum* [NiFe] hydrogenase in the oxidized state. **A** Ready enzyme. **B** Unready enzyme. The exact identity of the bridging oxygen ligand cannot be postulated based on the present data. Protons shown in *bold* can be exchanged in active, reduced enzyme. Numbering of the S atoms of the Cys residues is as in the *D. gigas* crystal structure [1]

on $Ni^{3+}$. These observations, and the fact that the $g_z$ line is very close to the free electron value, indicate that the unpaired electron is in an orbital with a large $d_{z2}$ character, i.e. the orbital pointing towards the apical halide. This supports our model of the $Ni_r$* active site in which an $OH^-$ is binding at the $Ni^{3+}$ ion in the direction of the *z*-axis and pointing towards the gas channel, rather than to the Fe atom (Fig. 4A).

ENDOR experiments with $^{57}Fe$-enriched enzyme from *Desulfovibrio desulfuricans* also indicated the absence of a bridging ligand in the ready state [28]; no coupling between the Ni-based unpaired spin and the Fe nucleus could be observed. The same study showed that in the $Ni_u$* state of the enzyme from *D. gigas* the electronic contact between the Fe and the Ni was a little stronger, since a weak coupling (~1 MHz) was observed.

From the magnitude of the anisotropic coupling the distance from the proton to the unpaired electron can be calculated. Assuming a completely anisotropic coupling of 2.35 G (6.6 MHz), we estimate a Ni-H distance of 1.7–2.3 Å. According to extended X-ray absorption fine structure (EXAFS) measurements on the *A. vinosum*

enzyme, the Ni-O distance in the $Ni_r$* state is 1.86 Å [29]. On average, O-H bonds are 1.0 Å long. Stereochemically these bond lengths require a bend coordination of the $OH^-$ to the Ni with a Ni-O-H angle of about 100° to fit the estimated distance (Fig. 4A). This is also in line with the weak $^{17}O$ interaction in the *z*-direction [11]; a much stronger interaction would be expected for a $^{17}O$ nucleus oriented along the *z*-axis.

An exchangeable proton at this position in the $Ni_u$* state is unlikely since in $H_2O$ and $D_2O$ the EPR spectra are the same and the splitting of the $g_z$ line by the $\beta$-$CH_2$ protons of the Cys533 is almost resolved. On basis of the crystal structure data we opt for an oxygen species in the bridging mode in the unready state (Fig. 4B). In the crystal structure (assuming to represent mainly the oxidized and reduced, unready states [1]) the oxygen is bridging in an asymmetric manner [4], the Ni-O distance being 1.7 Å and the Fe-O distance 2.1 Å [30]. However, final proof can only be obtained by comparing the crystal structures of the enzyme in the $Ni_r$* and $Ni_u$* states. This work is currently in progress.

After discussing the nature of the coupling protons H1, H2 and H4, we will now turn to H3. This shows a small (3.5 MHz), rather anisotropic, coupling in ENDOR spectra [13, 21] and the proton causing it (H3) could be exchanged after activation and re-oxidation of the enzyme [21]. Electron spin-echo envelope modulation (ESEEM) measurements also showed a coupling of an exchangeable proton after re-oxidation to the $Ni_u$* state [31]. Based on these literature data and the active site models derived from this study, we favour the proton H3 on one of the terminal Cys thiols. The exchangeability of this proton in the reduced, active enzyme implies that (de)protonation of this ligand might play a role in catalysis. On the basis of the different biochemical properties of [NiFeSe] hydrogenases compared to [NiFe] hydrogenases, we support the proposal that Cys530, which is replaced with a selenoCys residue in [NiFeSe] hydrogenases, acts as the proton-accepting base in catalysis [12]. This could be a proton which can be exchanged in both $Ni_u$* and in $Ni_r$* upon reduction and re-oxidation. EPR is not sensitive enough to sense a hyperfine coupling of this H3 proton (this study). ENDOR measurements on *A. vinosum* [NiFe] hydrogenase in the pure unready state prepared in $H_2O$ and $D_2O$ might yield more information about the nature of this proton.

## Reactivity of oxidized enzyme

The different active-site structures for the enzyme in the unready and the ready states provide a possible basis to understand the differences in reactivity. In the ready state the Fe atom is five coordinate, so dihydrogen can bind at the sixth site. We assume that this $H_2$ is subsequently used to reduce the Ni ion and the 3Fe cluster. This changes the p$K_a$ of the Ni-bound $OH^-$, which can be protonated and then removed from the active site as water. A second $H_2$ then binds to the Fe site, inducing the oxidation of $Ni^{2+}$ to $Ni^{3+}$ (the $Ni_a$-C* state). This state can rapidly react with another $H_2$ to form the fully reduced $Ni_a$-SR state [17, 32].

In the unready state a bridging oxygen species forms the sixth ligand to iron, thus preventing the binding of dihydrogen to iron and subsequent activation. We envisage the very slow conversion of the unready state to the ready state, which occurs under mildly reducing conditions at the one-electron reduced, EPR-silent level [2] as the rearrangement of the oxygen species bound to nickel from a bridging to an end-on position. This transition requires elevated temperatures for the *A. vinosum* enzyme (40–50 °C).

**Acknowledgements** The investigations were supported (in part) by EU grant no. BIO4-98-0280 and by the Netherlands Organization for Scientific Research (NWO), division for Chemical Sciences (CW). W. Roseboom is kindly acknowledged for general technical assistance and for the purification of the *A. vinosum* hydrogenase. Dr. R. Hedderich (Marburg, Germany) is acknowledged for the kind gift of the *M. marburgensis* hydrogenase.

## References

1. Volbeda A, Charon MH, Piras C, Hatchikian EC, Frey M, Fontecilla-Camps JC (1995) Nature 373:580–587
2. Surerus KK, Chen M, van der Zwaan JW, Rusnak F, Kolk M, Duin EC, Albracht SPJ, Münck E (1994) Biochemistry 33:4980–4993
3. Dole F, Fournel A, Magro V, Hatchikian EC, Bertrand P, Guigliarelli B (1997) Biochemistry 36:7847–7854
4. Volbeda A, Garcin E, Piras C, de Lacey AL, Fernandez VM, Hatchikian EC, Frey M, Fontecilla-Camps JC (1996) J Am Chem Soc 118:12989–12996
5. Happe RP, Roseboom W, Pierik AJ, Albracht SPJ, Bagley KA (1997) Nature 385:126
6. Pierik AJ, Roseboom W, Happe RP, Bagley KA, Albracht SPJ (1999) J Biol Chem 274:3331–3337
7. Krasna AI, Rittenberg D (1954) J Am Chem Soc 76:3015–3020
8. Albracht SPJ (1994) Biochim Biophys Acta 1188:167–204
9. Fernandez VM, Hatchikian EC, Cammack R (1985) Biochim Biophys Acta 832:69–79
10. Van der Zwaan JW, Albracht SPJ, Fontijn RD, Slater EC (1985) FEBS Lett 86:122–126
11. Van der Zwaan JW, Coremans JMCC, Bouwens ECM, Albracht SPJ (1990) Biochim Biophys Acta 1041:101–110
12. Garcin E, Vernede X, Hatchikian EC, Volbeda A, Frey M, Fontecilla-Camps JC (1999) Structure 7:557–566
13. Geßner Ch, Stein M, Albracht SPJ, Lubitz W (1999) JBIC 4:379–389
14. Van Heerikhuizen H, Albracht SPJ, Slater EC, Van Rheenen PS (1981) Biochim Biophys Acta 657:26–39
15. Hendley DD (1955) J Bacteriol 70:625–634
16. Albracht SPJ, Kalkman ML, Slater EC (1983) Biochim Biophys Acta 724:309–316
17. Coremans JMCC, Van Garderen CJ, Albracht SPJ (1992) Biochim Biophys Acta 1119:148–156
18. Beinert H, Albracht SPJ (1982) Biochim Biophys Acta 683:245–277
19. Niu S, Thomson LM, Hall MB (1999) J Am Chem Soc 121:4000–4007
20. De Gioia L, Fantucci P, Guigliarelli B, Bertrand P (1999) Inorg Chem 38:2658–2662
21. Fan C, Teixeira M, Moura J, Moura I, Huynh BH, Le Gall J, Peck HD Jr, Hoffman B (1991) J Am Chem Soc 113:20–24
22. Whitehead JP, Gurbiel RJ, Bagyinka C, Hoffman BM, Maroney MJ (1993) J Am Chem Soc 115:5692–5635

23. Trofanchuk O, Stein M, Geßner Ch, Lendzian F, Higuchi Y, Lubitz W (2000) JBIC 5:36–44
24. Montet Y, Amara P, Volbeda A, Vernede X, Hatchikian EC, Field MJ, Frey M, Fontecilla-Camps JC (1997) Nat Struct Biol 7:523–526
25. Ogata H, Mizuno N, Miki K, Adachi S, Yasuoka N, Yagi T, Higuchi Y (2000) Results presented at the 6th international conference on the molecular biology of hydrogenases, Potsdam, Germany
26. Grove DM, van Koten G, Zoet R, Murall NW, Welch AJ (1983) J Am Chem Soc 105:1379–1380
27. Wertz JE, Bolton JR (1972) Electron spin resonance, elementary theory and practical applications. Chapman and Hall, New York
28. Huyett JE, Carepo M, Pamplona A, Franco R, Moura I, Moura JJG, Hoffman BM (1997) J Am Chem Soc 119:9291–9292
29. Davidson G, Choudhury SB, Gu Z, Bose K, Roseboom W, Albracht SPJ, Maroney MJ (2000) Biochemistry 39:7468–7479
30. Fontecilla-Camps JC, Ragsdale SW (1999) Adv Inorg Chem 47:283–333
31. Chapman A, Cammack R, Hatchikian CE, McCracken J, Peisach J (1988) FEBS Lett 242:134–138
32. Happe RP, Roseboom W, Albracht SPJ (1999) Eur J Biochem 259:602–608